Dynamics of $A + B \rightarrow C$ Reaction Fronts in the Presence of Buoyancy-Driven Convection

L. Rongy, P. M. J. Trevelyan, and A. De Wit

Nonlinear Physical Chemistry Unit, CP 231, Faculté des Sciences, Université Libre de Bruxelles (ULB), 1050 Brussels, Belgium

(Received 27 March 2008; published 22 August 2008)

The dynamics of $A + B \rightarrow C$ fronts in horizontal solution layers can be influenced by buoyancy-driven convection as soon as the densities of A, B, and C are not all identical. Such convective motions can lead to front propagation even in the case of equal diffusion coefficients and initial concentration of reactants for which reaction-diffusion (RD) scalings predict a nonmoving front. We show theoretically that the dynamics in the presence of convection can in that case be predicted solely on the basis of the knowledge of the one-dimensional RD density profile across the front.

DOI: 10.1103/PhysRevLett.101.084503 PACS numbers: 47.70.Fw, 47.20.Bp, 82.40.Ck

When separate solutions of chemicals A and B, reacting according to the simple kinetic scheme $A + B \rightarrow C$, are brought into contact, a reaction front, i.e., a spatially localized region with nonzero production rate, is formed. The RD properties of such fronts have been thoroughly studied due to their ubiquitous appearance in physical, biological, and chemical systems. In particular, the pioneering work of Gálfi and Rácz [1] and subsequent other theoretical approaches [2–4] have considered the scalings of the one-dimensional (1D) RD profiles when A and B (with diffusion coefficients D_a and D_b, respectively) meet with initial concentrations a_0 and b_0, respectively. It has been shown that the reaction front position x_f (defined as the location of maximum production rate) moves if one of the reactants is in excess and/or the two reactants have different diffusion coefficients (i.e., if $a_0^2 D_a \neq b_0^2 D_b$) [1–4]. In that case, x_f scales for large times as $t^{1/2}$ while the reaction front width scales as $t^{1/6}$. The reaction front speed depends then on the ratio b_0/a_0 but not on the magnitudes of a_0 and b_0. Experimental work on reactions of the form $A + B \rightarrow C$ in gels both validate these RD scalings and quantitatively agree with the theoretically predicted positions of the reaction front [5,6].

However, these RD predictions break down if buoyancy effects due to differences in density of A, B, and C come into play. As an example, the reaction studied in [6] was next examined by Park *et al.* [7] in the absence of a gel in a solution contained between two horizontal slides separated by a narrow gap. Their results show a discrepancy with the theoretically predicted RD front positions and an experimental front traveling faster, effects likely due to buoyancy-induced convection. Deviations from the classical RD theories have further been made evident recently by Shi and Eckert [8] in their experimental study of an acid-base reaction front propagation in a horizontal Hele-Shaw cell. They found that the front position still scales asymptotically as $\sqrt{t}$. However, the front travels faster when the gap width of the cell is increased and its speed depends on the initial concentrations at fixed ratio b_0/a_0. The larger the initial concentrations, the faster the front moves, an observation pointing to the influence of increasing convection related to buoyancy effects.

Even though the effect of such buoyancy-driven flows upon autocatalytic RD fronts has been extensively investigated experimentally and numerically (see [9,10] and references therein), no equivalent analyses have been devoted until now to the case of the simpler $A + B \rightarrow C$ fronts.

In this context, it is the objective of this Letter to analyze by a theoretical approach the influence of buoyancy-driven convection on the properties of $A + B \rightarrow C$ fronts. To do so, we numerically solve Stokes equations coupled to reaction-diffusion-convection (RDC) equations for the concentrations a, b, c of the reactants A, B, and of the product C in the case $a_0 = b_0$ with equal diffusion coefficients. The dynamics are classified as a function of the Rayleigh numbers $R_{a,b,c}$ of the species A, B, C. We show that natural convection dramatically affects the problem and invalidates the RD properties. Fortunately, a correlation between the numerical results and analytical inspection of the density profile across the front shows that the RDC dynamics can be fully predicted solely on the basis of the knowledge of the Rayleigh numbers of the problem.

We consider a two-dimensional solution layer oriented horizontally with z pointing upwards in the gravity field $\underline{g}$ and x horizontal, in which the $A + B \rightarrow C$ reaction takes place upon contact between two solutions each containing one of the reactants. The governing RDC equations are coupled to the 2D incompressible Stokes equations for the velocity field $\underline{v}$ by a state equation for the solution density ρ assumed to depend linearly on the concentrations as

$$\rho = \rho_0 + \frac{\partial \rho}{\partial a} a + \frac{\partial \rho}{\partial b} b + \frac{\partial \rho}{\partial c} c, \tag{1}$$

where ρ_0 is the density of the solvent and $\partial \rho / \partial c_i$ the solutal expansion coefficient of species i. The dynamic viscosity μ, chemical rate constant k, and diffusion coefficients $D_{a,b,c}$ of species A, B, and C, are assumed constant.

Dimensionless equations are obtained by using the characteristic RD scales: time $\tau_c = 1/k a_0$, length $L_c = \sqrt{D_a \tau_c}$,

velocity $U_c = \sqrt{D_a/\tau_c}$, pressure $p_c = \mu/\tau_c$, and for concentration, a_0. Defining a dimensionless pressure gradient which includes the hydrostatic term, we obtain the dimensionless governing equations with $\underline{\nabla} \cdot \underline{v} = 0$:

$$\frac{\partial a}{\partial t} + \underline{v} \cdot \underline{\nabla} a = \nabla^2 a - ab, \tag{2}$$

$$\frac{\partial b}{\partial t} + \underline{v} \cdot \underline{\nabla} b = \delta_b \nabla^2 b - ab, \tag{3}$$

$$\frac{\partial c}{\partial t} + \underline{v} \cdot \underline{\nabla} c = \delta_c \nabla^2 c + ab, \tag{4}$$

$$\underline{\nabla} p = \nabla^2 \underline{v} - (R_a a + R_b b + R_c c)\underline{i}_z, \tag{5}$$

where $\delta_{b,c} = D_{b,c}/D_a$ and $\underline{i}_z$ is the unit vector along z. The dimensionless Rayleigh numbers $R_{a,b,c}$ are defined as

$$R_i = \frac{\partial \rho}{\partial c_i} \frac{a_0 g L_c^3}{\mu D_a}, \tag{6}$$

where c_i is the dimensionless concentration of the relevant species and $g = |\underline{g}|$. The Rayleigh numbers $R_{a,b,c}$ are positive because the solutes are all supposed to increase the density of water. We require zero-flux boundary conditions for the concentrations and no-slip boundary conditions for $\underline{v}$. The initial conditions are separated reactants such that for all z, $(a, b, c) = (1, 0, 0)$ for $x < 0$ while $(a, b, c) = (0, 1, 0)$ for $x > 0$. To highlight the influence of convection, the initial concentrations are chosen as equal ($a_0 = b_0$) and all species are set to diffuse at the same rate, i.e., $\delta_b = \delta_c = 1$. In that case, the RD front is stationary (i.e., $x_f = 0$ in the course of time) in the absence of convection [1–4]. Numerical simulations of Eqs. (2)–(5) are carried out in a domain of height L_z and width L_x using the numerical procedure described in [10]. The width was chosen sufficiently large that the solutions are unaffected by boundary effects along the x direction. The domain height, L_z, affects all of the quantitative scalings in this problem but is qualitatively not important for the parameters investigated here.

The RDC dynamics depends on the relative values of the densities $\rho_i = R_i c_i$ of the three species A, B, and C involved. In Fig. 1, density plots of a, b, c, and production rate ab are illustrated for the case where species C is the least dense and so rises to the top, while the more dense A and B sink to the bottom. This generates a strong convective roll turning clockwise on the right where B sinks below C and a second shorter and weaker counterclockwise convective roll on the left where A sinks below C [Fig. 2(a)]. The asymmetry in the intensity of convection and in the deformation of the concentration fields is due to the fact that the density difference between B and C is here larger than between A and C. This asymmetry yields a global acceleration to the left as seen in Figs. 1 and 2(a) superimposing velocity vectors on a density plot of the production rate ab. In Fig. 2(b), the density of C in the reaction zone is intermediate to that of the reactants. A single standing convective roll is present and turns clockwise as the heavier B is sinking below A and C. In Fig. 2(c), the density of C is further increased. Now there are again two convective rolls, a strong clockwise convective roll on the left and a shorter and weaker counterclockwise roll on the right giving a global acceleration to the right. This situation

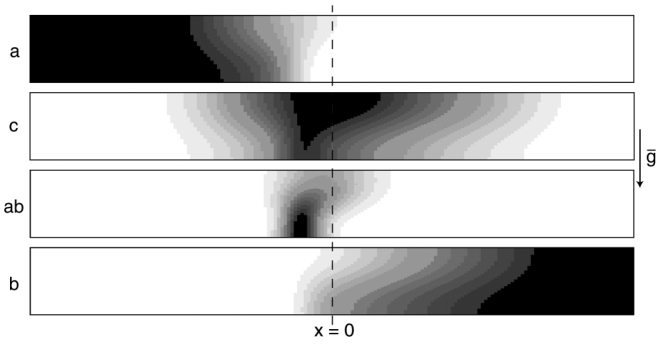

FIG. 1. Density plots of a, c, b, and production rate ab focusing on the reaction zone at time $t = 50$ for $R_a = 2$, $R_b = 4$, and $R_c = 1$ with $L_x = 90$ and $L_z = 10$. Dark regions correspond to high concentrations.

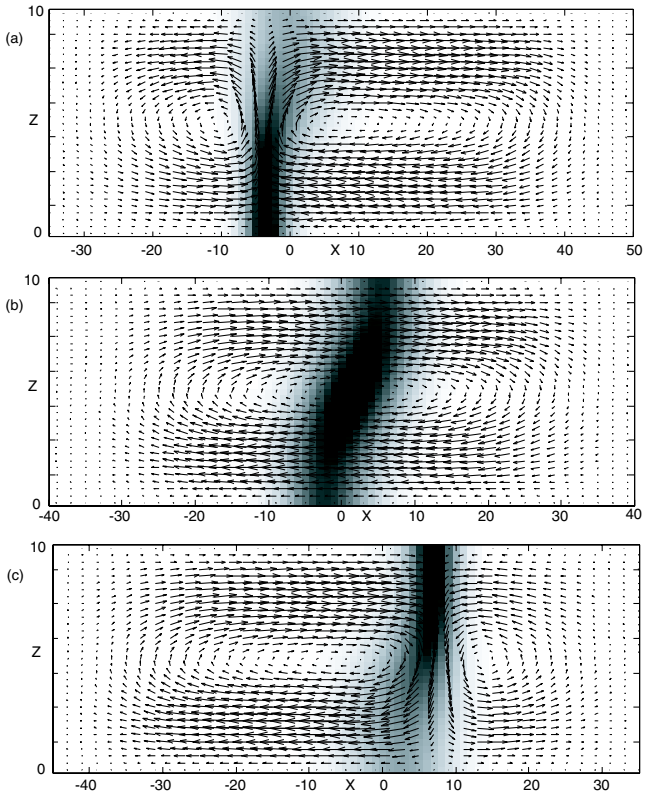

FIG. 2 (color online). Fluid velocity field superimposed on the density plots of the production rate ab at time $t = 50$ for $R_a = 2$ and $R_b = 4$ with (a) $R_c = 1$, (b) $R_c = 6$, and (c) $R_c = 10$. $x = 0$ denotes the initial position of the front and gravity points downwards.

is the opposite to that in Fig. 2(a) since C is now the heaviest species. The maximum production rate is localized where the two convective rolls meet in Figs. 2(a) and 2(c) and in the middle of the single convective roll in Fig. 2(b).

We recall that the position of the reaction front x_f is defined in 1D RD systems by the location of the point where the production rate is maximum. However, two coordinates x and z are needed to localize such a point in the RDC dynamics because of convective front deformation in the height of the layer. We define therefore here the front position X_f as the point where the vertically averaged production rate reaches its maximum in order to compare with the 1D RD value x_f [11]. X_f takes negative, zero, or positive values, respectively, in Figs. 2(a)–2(c), although the RD analysis predicts that this position should not move ($x_f = 0$) when the two reactants diffuse at the same rate and have initially the same concentrations as in the present analysis [1].

A close examination of the RDC dynamics for various sets of Rayleigh numbers shows that the number of convective rolls, their relative size, and rotational direction can all be predicted on the basis of the 1D RD density profile. Indeed, as the flow field is driven by the density gradient, we find that two convective rolls are present when the density profile $\rho(x, t)$ is nonmonotonic, i.e., its gradient $\rho_x(x, t)$ changes sign in the x direction. On the contrary, only a single convective roll is present when $\rho(x, t)$ is monotonic, i.e., its gradient is single signed.

This monotonic feature of $\rho(x, t)$ is independent of time and can actually be predicted from the simple 1D RD concentration profiles and from the values of the Rayleigh numbers. Indeed, as we have equal diffusion coefficients with initially equal concentrations, the appropriate sums of Eqs. (2)–(4) with $\underline{v} = \underline{0}$ and with the initial conditions show that $a + b + 2c = 1$ for all times. Thus, $c(x, t) = \frac{1}{2}[1 - a(x, t) - b(x, t)]$. This allows the density $\rho = R_a a + R_b b + R_c c$ to be reconstructed and taking its derivative with regard to x, we obtain

$$\rho_x(x, t) = \left(R_a - \frac{R_c}{2}\right)a_x(x, t) + \left(R_b - \frac{R_c}{2}\right)b_x(x, t). \quad (7)$$

As the gradients of a and b are single signed with $a_x \leq 0$ and $b_x \geq 0$, ρ_x is single signed when R_c lies between $2R_a$ and $2R_b$. Further, as the concentration of a and b are not symmetric about the reaction front, ρ_x will change sign whenever R_c lies outside the range between $2R_a$ and $2R_b$. In Fig. 3, a sketch of the 6 different possible types of density profiles are illustrated in the $R_b - R_c$ plane at fixed R_a. The shaded regions corresponding to $2R_a < R_c < 2R_b$ or $2R_b < R_c < 2R_a$ have monotonic density profiles yielding fluid flows with only one convective roll. This single vortex turns clockwise when $R_b > R_a$, i.e., when heavy B sinks below lighter A and counterclockwise when $R_b < R_a$.

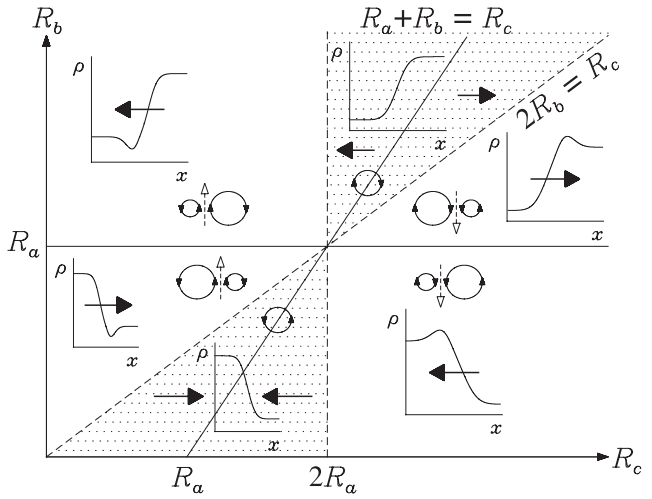

FIG. 3. Classification of the different RDC dynamics in the (R_b, R_c) parameter plane at fixed R_a. Typical density profiles in the absence of convection as well as a sketch of the expected vortex dynamics are illustrated within the corresponding regions. The shaded region corresponds to monotonic density profiles with one single vortex. Outside the shaded region, nonmonotonous density profiles and two vortices are obtained. The arrow on the circles indicate the rotation direction of the vortex. The dashed arrow indicates whether C is rising or sinking in the gravity field while the dark filled arrow shows the initial direction of propagation of the front.

The unshaded regions feature nonmonotonic density profiles for which two convective rolls are observed.

When $R_c = R_a + R_b$, the loss in density by the consumption of a and b in the reaction is equal to the gain in density by the production of c so that the density profile is antisymmetric with regard to $x = 0$, i.e., the density gradient is symmetric: $\rho_x(x, t) = \rho_x(-x, t)$. On the basis of Eq. (7) and noting that, from symmetry, we have $b(x, t) = a(-x, t)$, this property implies that $(R_a + R_b - R_c) \times [a_x(x, t) - a_x(-x, t)] = 0$ which confirms that $R_c = R_a + R_b$ yields an antisymmetric density profile. When $R_b = R_a$, the reactants A and B have equal densities with either lighter or heavier C so that the density profiles along x (both in the absence and in the presence of convection) are symmetric. In those two cases, denoted by the solid lines in Fig. 3, the front remains stationary ($X_f = 0$) even if convection is present in the system. The strength of this convection decreases when one approaches the peculiar point $R_c = 2R_a = 2R_b$ where the density is constant everywhere, no fluid flow is obtained ($\underline{v} = \underline{0}$), and the planar RD stationary front with $X_f = 0$ is recovered. For any values of R_a, R_b, R_c outside of the 2 solid lines, the density profile is asymmetric along x, giving rise to asymmetric convection. This results in the propagation of the front in the opposite direction of the most intensive fluid flow which is located at the left ($x < 0$) or at the right ($x > 0$) depending whether the density jump between the solution of C and, respectively, the solution of A or B is the

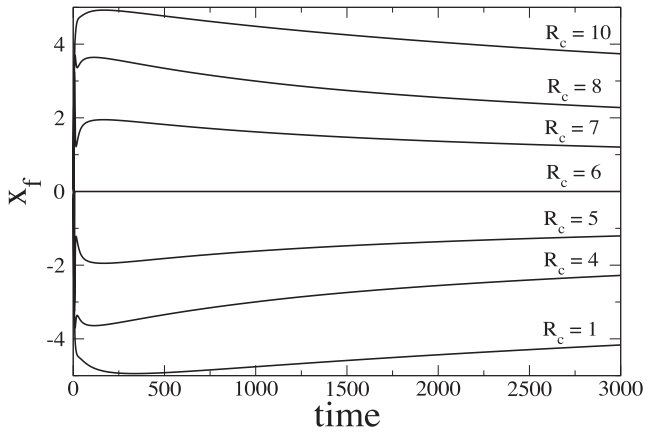

FIG. 4. X_f against time with $R_a = 2$ and $R_b = 4$ for various values of R_c.

largest. Hence, when $R_b > R_a$, the reaction front moves to the right if $R_c > R_a + R_b$ (the strongest fluid flow is on the left) and to the left if $R_c < R_a + R_b$ (the strongest fluid flow is on the right). The reverse is true when $R_b < R_a$. When two vortices are present, their relative strength depends on the relative position with regard to the horizontal line $R_b = R_a$. When $R_b > R_a$, the strongest roll located at the side where the density jump between one of the reactant and C is the largest rotates clockwise while it turns counterclockwise when $R_b < R_a$. When $R_b = R_a$, both rolls are of the same size and strength (and hence $X_f = 0$) since the reactants A and B have equal densities with lighter C rising in the middle if $R_c < R_a + R_b = 2R_a$ and heavy C sinking otherwise.

To sum up part of the predictions of Fig. 3, X_f is plotted in Fig. 4 against time with $R_a = 2$ and $R_b = 4$ for various values of R_c. When $R_c = 6$, i.e., on the line $R_c = R_a + R_b$, the front remains effectively stationary with $X_f = 0$ as explained above. As $R_b > R_a$, the front moves to the left ($X_f < 0$) for $R_c < R_a + R_b = 6$ and to the right ($X_f > 0$) when $R_c > 6$.

Finally, Fig. 4 indicates that, in the course of time, the driving force of convection decreases as the density gradients are weakening. Hence, the reaction front slows down and changes direction to return at infinite time to its initial position $X_f = 0$ (diffusive limit predicted by Gálfi and Rácz [1]) while the convective deformations shown in Fig. 1 decrease in time. Notice that this change in direction of the reaction front due to a weakening in time of convection vs diffusion has nothing to do with the change in direction of a pure RD front observed for unequal diffusion coefficients and initial concentrations [12].

To conclude, as soon as density asymmetries exist across an $A + B \rightarrow C$ reaction front, buoyancy-driven convection sets in and leads to a global movement of the front in the direction of the smallest density gradient. This occurs even if A and B have equal diffusion coefficients and initial concentrations in which case the RD front remains immobile. Fortunately, the whole RDC dynamics can in that case be predicted solely on the basis of the 1D RD density profiles across the front. Thus, a simple experimental measure of the solutal expansion coefficient (and hence of the Rayleigh number) of each chemical species is in practice sufficient to reconstruct the 1D density profile and to predict (see Fig. 3) whether one or two convection rolls will be present and whether the front will be convected to the left or to the right. Unfortunately, comparison with available experimental data in absence of gels [7,8] is not possible yet. Values of solutal expansion coefficients are not given in Park *et al.*'s experiments [7] while diffusion coefficients are not equal in the system of Shi and Eckert [8]. However, we hope that the simplicity of the experimental methodology suggested here to test our theoretically predicted RDC dynamics will trigger new experiments on $A + B \rightarrow C$ in simple horizontal covered solution layers. From a theoretical point of view, a parametric study of the intensity of the convective acceleration of the fronts and of its influence on the classical RD scaling needs now to be undertaken to allow for comparison with foreseen experiments done in the absence of gels. Eventually, let us note that for unequal diffusion coefficients with unequal initial concentrations, there are 32 different types of density profiles. A first inspection shows that acceleration and reversal of the front propagation direction in time can be obtained in some situations.

We thank K. Eckert for fruitful discussions and Prodex, FNRS, and the Communauté française de Belgique for financial support. L. R. received additional support from FNRS and P. M. J. T. from the PRODEX program of ESA.

[1] L. Gálfi and Z. Rácz, Phys. Rev. A **38**, 3151 (1988).
[2] Z. Jiang and C. Ebner, Phys. Rev. A **42**, 7483 (1990).
[3] S. Cornell, Z. Koza, and M. Droz, Phys. Rev. E **52**, 3500 (1995).
[4] Z. Koza, J. Stat. Phys. **85**, 179 (1996).
[5] Y.-E. L. Koo, L. Li, and R. Kopelman, Mol. Cryst. Liq. Cryst. **183**, 187 (1990).
[6] Y.-E. L. Koo and R. Kopelman, J. Stat. Phys. **65**, 893 (1991).
[7] S. H. Park *et al.*, Phys. Rev. E **64**, 055102(R) (2001).
[8] Y. Shi and K. Eckert, Chem. Eng. Sci. **61**, 5523 (2006).
[9] J. A. Pojman and I. R. Epstein, J. Phys. Chem. **94**, 4966 (1990).
[10] L. Rongy, N. Goyal, E. Meiburg, and A. De Wit, J. Chem. Phys. **127**, 114710 (2007).
[11] Similar results are obtained if X_f is defined as the position along x of the global maximum of the production rate.
[12] H. Taitelbaum *et al.*, Phys. Rev. A **46**, 2151 (1992).